Research Article | Vol. 29, No. 16 / 2 August 2021 / Optics Express 26014
Optics EXPRESS

Absolute frequency readout derived from ULE cavity for next generation geodesy missions

EMILY ROSE REES,[1,2,*] ANDREW R. WADE,[1,2] ANDREW J. SUTTON,[1,2] ROBERT E. SPERO,[3] DANIEL A. SHADDOCK,[1,2] AND KIRK MCKENZIE[1,2]

[1] *Centre for Gravitational Astrophysics (CGA), Research School of Physics, The Australian National University, Canberra ACT 2601, Australia*
[2] *ARC Centre of Excellence for Gravitational Wave Discovery (OzGrav), Research School of Physics, The Australian National University, Canberra ACT 2601, Australia*
[3] *Jet Propulsion Laboratory (JPL), California Institute of Technology, 4800 Oak Grove Drive Pasadena, CA 91109, USA*
[*] *emilyrose.rees@anu.edu.au*

Abstract: The next generation of Gravity Recovery and Climate Experiment (GRACE)-like dual-satellite geodesy missions proposals will rely on inter-spacecraft laser interferometry as the primary instrument to recover geodesy signals. Laser frequency stability is one of the main limits of this measurement and is important at two distinct timescales: short timescales over 10-1000 seconds to measure the local gravity below the satellites, and at the month to year timescales, where the subsequent gravity measurements are compared to indicate loss or gain of mass (or water and ice) over that period. This paper demonstrates a simple phase modulation scheme to directly measure laser frequency change over long timescales by comparing an on-board Ultra-Stable Oscillator (USO) clocked frequency reference to the Free Spectral Range (FSR) of the on-board optical cavity. By recording the fractional frequency variations the scale correction factor may be computed for a laser locked to a known longitudinal mode of the optical cavity. The experimental results demonstrate a fractional absolute laser frequency stability at the 10 ppb level (10^{-8}) at time scales greater than 10 000 seconds, likely sufficient for next generation mission requirements.

The Gravity Recovery and Climate Experiment (GRACE) missions [1,2] track *localized* changes in Earth's gravity field over months and years. These fluctuations in the local gravity field are representative of mass transport processes, and are primarily driven by hydrological changes: the accumulation and melting of ice, changes in ground water levels through seasonal variation and extraordinary events such as drought. The importance of such data has led to significant interest within the Earth Science community, ranking GRACE-like missions as one of the top priorities [3]. Emphasis has been placed on the need for continuity of data and improvements to sensitivity going forward. Future GRACE-like missions, including NASA's Mass-Change mission study [4] and the Next-Generation Gravity Mission [5], are in the planning phase but expected to launch in the mid-2020's to achieve continuity with GRACE Follow-On [2].

In GRACE-like missions, two identical satellites are placed into an approximately 500 km altitude near-polar orbit (89°) with a separation of 220 km. Inter-spacecraft ranging is used to precisely track the relative satellite separation at micrometer precision or better. When combined with GPS location and on-board accelerometer measurements (to remove atmospheric drag), the gravitational variations on the Earth can be inferred with spatial resolution of about 300 km. Global maps of Earth's gravitational changes are published monthly, revealing the motion of water on the Earth due to local, seasonal and climatic changes over years and decades. GRACE (2002) and GRACE Follow-On (GRACE-FO, 2018) used K/Ka-Band microwave ranging for

#434483 https://doi.org/10.1364/OE.434483
Journal © 2021 Received 18 Jun 2021; revised 12 Jul 2021; accepted 12 Jul 2021; published 28 Jul 2021

Optics EXPRESS

their primary science, however GRACE-FO included a Laser Ranging Interferometer (LRI) technology demonstration [6]. The GRACE-FO LRI met all of the technology goals and has been producing scientific quality data for the mission. Recent work shows that the higher precision and lower noise of the LRI system can reveal new insights [7] and this trend is expected to continue. At a sensitivity noise floor of approximately 10 nm/$\sqrt{\text{Hz}}$ [6], it resolved range some two orders of magnitude better than the primary Microwave Instrument equivalent [2]. This improved sensitivity makes a LRI the leading choice for primary instrument selection on next generation gravity sensing missions.

To qualify a LRI as the prime and only inter-spacecraft ranging measurement for the next mission, NASA's Mass Change Study [4] identifies three areas requiring further work: increased robustness to thruster activation, system redundancy, and development of a method to read out the LRI Scale Correction or 'scale factor' to correct for long term drifts in laser frequency. Of these three items, the latter is the only new technology item. Without a Microwave Instrument on board, the LRI requires a new technique to mitigate the effect of laser frequency drift over timescales of a month and longer. The final mission requirement for absolute knowledge of the laser frequency is not decided but it is expected to demand fractional sensitivity on the order of 10 ppb (10^{-8}) or better [4,8].

This paper provides a detailed investigation of a 'scale-factor' measurement technique described in the Mass Change study, first developed at NASA/JPL [4] based on an extension of a proposal by Devoe and Brewer [9]. The scheme directly compares the frequency stability of an RF source, such as an on-board Ultra-Stable Oscillator (USO), against the mode spacing (c/2L) of an optical cavity. The experimental results demonstrate a fractional absolute laser frequency stability at about 1 ppb (10^{-9}), likely sufficient for next generations mission requirements.

The inclusion of such a technique in the next GRACE mission is predicated on two important factors: a relatively simple implementation requiring only low risk changes to flight-heritage LRI hardware, and that the addition of the scale-factor measurement does not compromise the short-term laser frequency stability demonstrated by the LRI on orbit. This paper addresses both factors, presenting a possible configuration for integration into the mission and a demonstration of unaffected laser stability at the short timescales.

The paper is laid out as follows; in Section 1 the motivation for the scale-factor is introduced. Sections 2 and 3 introduce the concept and a specific implementation that may be useful for future space missions. Section 4 presents an experimental demonstration and results of this concept using optical cavities and lasers.

1. Motivation for the scale-factor measurement

The GRACE-FO mission reports a scale-correction, $\epsilon(t)$, to correct for laser frequency change over time [10], derived by comparing the microwave and laser ranging measurements. This scale factor is of critical importance in calibrating measurements for monthly and yearly gravity maps, where changes of laser frequency can be misinterpreted as a change in gravity. The sampled phase of individual samples at the same ground position will include contributions from the standing static gravity field as well as changes due to the movement of mass (mainly water). In order to meet the mission requirements the LRI laser must remain within a certain fractional frequency band in order for the residual month-to-month change signals to not be masked by the static gravity signal being scaled into the measurement.

On the GRACE Follow-On mission, the scale factor for the LRI is calculated from the residual difference between the microwave and laser range measurements. The microwave frequency is derived from on-board Ultra-Stable Oscillators (USO), and is known with very high accuracy (10^{-11} per day [11]). The laser frequency stability ($<10^{-13}$) significantly exceeds that of the USO over shorter timescales (10-1000 seconds [12]) by referencing and stabilizing its optical frequency against a resonant optical mode within an Ultra-Low Expansion (ULE) glass cavity. At

Optics EXPRESS

longer timescales the cavity length systematically drifts, influenced by the spacecraft temperature and aging of the glass, which results in a corresponding drift of laser absolute frequency. The time-varying laser frequency, ν, can be related to the initial laser frequency, $\nu_0 = 2.8 \times 10^{14}$[Hz], by the scale-factor $\nu = (1 + \epsilon(t))\nu_0$.

Such an un-calibrated, slow change in the laser frequency degrades the subtraction of the large static gravity signal, $S(f)$, from the science data when two time separated measurements are subtracted, as given by the following equation:

$$\Delta L_{\text{Scaling Noise}} = S(f)\frac{\nu_\sigma(\tau)}{\nu_0}. \tag{1}$$

Here one can write the laser absolute frequency as a mean value plus some statistical variation at measurement time separation τ, $\nu_i = \nu_0 + \nu_\sigma(\tau)$. Figure 1 shows the nominal range measurement, represented as a range spectral density, extracted from the GRACE Follow-On LRI on-orbit data, along with the laser frequency displacement noise requirement. The blue curve shows that the residual coupling of the static gravitational field for a scale-factor error $\epsilon = 10^{-8}$. At this level the coupling of static signal induced by a scale-factor error is smaller than the LRI instrument requirement, except at the once- and twice-per-orbit tone frequencies (0.18 mHz and 0.36 mHz). This error is likely sufficient for the next GRACE-like mission and, thus, for this article we estimate the scale factor accuracy requirement to be $\epsilon = 10^{-8}$. We define the requirement in terms of fractional laser frequency change as an Allan Deviation over the time scale 10 000 seconds and above as

$$\frac{\nu_\sigma(\tau)}{\nu_0} = 10^{-8}, \text{ for } \tau > 10\,000 \text{ seconds}. \tag{2}$$

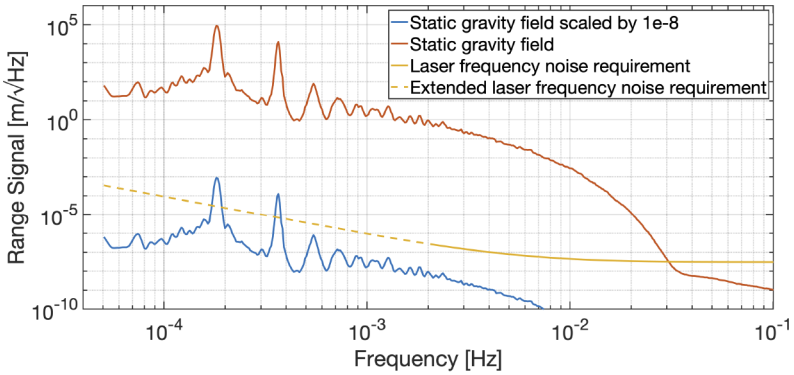

Fig. 1. The static gravity field amplitude spectral density measured by the LRI from Abich et al. [6] (red trace). The laser frequency noise requirement for GRACE Follow-On was 30 nm/$\sqrt{\text{Hz}}$ × NSF(f) (yellow solid trace). The scale factor correction produced by the GRACE-FO mission is on the order of 1.2e-7 [13] and derived by comparing the stabilised microwave system to the laser. The required error in the scale factor for the next GRACE mission is expected to be less than 10^{-8}, with the corresponding residual range error shown by the blue trace.

2. Scale factor measurement system for the next GRACE mission

To directly readout the scale factor in a future laser-only ranging instrument, it is necessary to develop a technique that can tie the absolute frequency of the laser light to an external reference, such as an iodine absorption line [4] or a USO [5]. With a view to minimizing changes to the LRI flight-heritage (NASA TRL9) hardware, such an approach should leverage existing LRI

Optics EXPRESS

resources wherever possible. We demonstrate a concept to sample the frequency spacing of the optical reference cavity with existing resources; a single laser, a single phase modulator and a single Megahertz bandwidth photoreceiver. The concept relies upon the fixed relationship of the laser's absolute frequency, ν_{Laser}, with the cavity longitudinal mode spacing, ν_{FSR}, when the laser is locked onto a specific resonant mode.

The scheme applies an optical phase modulation to infer the laser frequency change (or scale-factor) over long timescales by directly comparing the frequency stability of a reference oscillator to the Free Spectral Range (FSR) of an on-board optical cavity. In addition to a conventional PDH lock of the laser to a cavity resonant mode [14], the technique multiplies up an Ultra-Stable reference Oscillator (USO) signal from ≈ 38.66 MHz to coincide with the LRI flight cavity's FSR of ≈ 1.94 GHz and modulates this signal onto the phase of the light incident on the optical cavity. The modulation signal generates frequency-shifted optical sidebands which interact with the adjacent cavity resonant modes. Readout of any frequency difference between the actual cavity FSR and the generated Gigahertz sidebands uses a lock-in modulation-demodulation technique at a few Megahertz to give a PDH-like detuning readout, all using only a Megahertz bandwidth photodetector.

Locking the laser to a cavity resonance sets the laser frequency to be an integer multiple (n_{mode}) of the cavity longitudinal mode spacing frequency, the Free-Spectral Range (FSR) $\nu_{\text{FSR}} = c/2L \approx 1.94$ GHz, where L is the absolute cavity length and c the speed of light in vacuum. Accordingly, the laser's optical frequency and FSR are related by the mode number $n_{mode} \equiv \nu_{\text{Laser}}/\text{FSR}$. Feedback locking then ensures that changes in cavity length δL are proportionally replicated in both laser frequency and cavity FSR, $\delta L/L = \delta\nu_{\text{Laser}}/\nu_{\text{Laser}} = \delta\nu_{\text{FSR}}/\nu_{\text{FSR}}$.

Calibration of the mode number n_{mode} prior to launch allows conversion of fractional frequency changes of the cavity FSR into a real time absolute frequency change by $\nu_{\text{Laser}} = n_{mode} \times \nu_{FSR}\,[Hz]$. Thus, with a minimum number of components, the proposed RF measurement of the cavity FSR is able to infer the scale factor using only local measurements on-board a single satellite, with measurement of the on-board USO's frequency drift calculated after data down-link by referencing GPS time measurements.

Figure 2 shows the current PDH laser locking scheme implemented on the GRACE Follow-On LRI, with the addition of the proposed Scale Factor Unit (SFU) electronics/hardware and associated FSR Firmware block diagram components. On the GRACE Follow-On LRI, the PDH locking scheme running on the Laser Ranging Processor (LRP) [12] directly drives a 1.5 MHz modulation into the phase modulator and uses a digital demodulation of the reflected photodetector signal from a cavity to derive a feedback signal [15][16].

The proposed SFU generates and adds a second modulation tone onto the LRP PDH signal prior to the Phase Modulator. The tone frequency is configured by the OBC to match the estimated FSR frequency ($\Upsilon_{FSR} \approx \nu_{FSR}$ [Hz]). A Megahertz phase modulation of the Gigahertz FSR tone provides a lock-in error signal sensitive to the difference between the actual and estimated cavity FSR frequency, as compared against the USO. The proposed readout closely mirrors the LRP's digital PDH lock-in implementation, including use of a common photodetector-digitizer chain, and allows for either closed- or open-loop correction of the FSR estimate from within the LRP or via ground telemetry. Required modifications to legacy-LRI hardware include an additional hardware-based frequency synthesizer to multiply the USO frequency up to the FSR frequency(~2 GHz), a Gigahertz bandwidth phase modulator in place of the current 150 MHz bandwidth device, additional digital lock-in readout implemented in the firmware of the LRP, and power, telemetry, and USO interfaces for the FSR readout electronics to interface with the spacecraft.

Optics EXPRESS

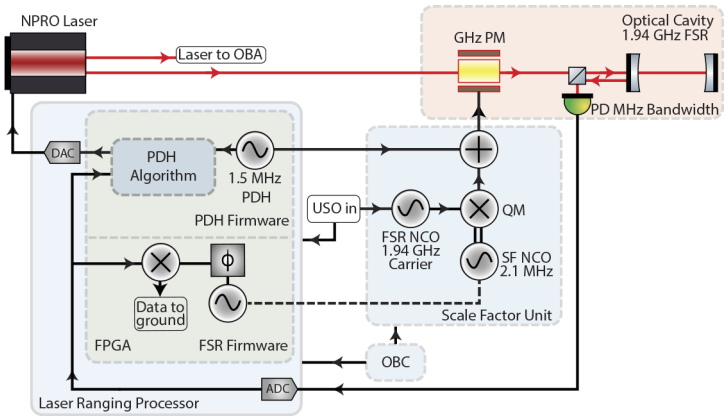

Fig. 2. Showing a possible block diagram for the laser sub-system of a future MCM mission, where scale-factor (SF) and PDH firmware are operated from a single FPGA. The laser has two output ports; the first is routed to the Optical Bench Assembly (OBA) which implements the inter-satellite interferometer link, while the second is routed to the optical cavity for laser frequency stabilization. The scale-factor measurement requires a new external unit, the Scale-Factor Unit (SFU), to implement the FSR Numerically Controlled Oscillator (NCO) for generation of the scale-factor measurement's Gigahertz tone (matched to the cavity FSR) and analog summation with the LRP's PDH modulation signal. The FSR tone is phase modulated using a Quadrature Mixer (QM) by the output of a second NCO, the Scale-Factor NCO (SF NCO), which generates a Megahertz modulation used to sense changes in cavity FSR. The LRP's FSR firmware implements lock-in detection at the SF NCO's phase modulation frequency (Υ_{SF}) for readout of cavity FSR changes. The dashed line linking the LRP FSR firmware with the SF NCO represents an optional phased synchronization which may simplify lock-in detection. The configuration shown here is an open-loop readout, whereby the changes in FSR are sent to ground as part of regular telemetry data. This scheme permits regular/periodic updates to the estimated FSR by a ground-to-satellite parameter upload, or an alternate software-based closed loop feedback to the Scale Factor Unit's FSR oscillator frequency via communication with the satellite On-Board Computer (OBC).

3. Cavity FSR readout

This section presents a derivation of the lock-in Scale Factor readout scheme detailed in the previous section. At a high level, the measurement relies upon generation of frequency-offset sub-carriers to sense the frequency-spacing of optical cavity resonances above and below the PDH resonant mode. Sub-carriers are generated by the *FSR tone* applied as phase modulation prior to the cavity at a frequency approximating the FSR $\Upsilon_{FSR} \approx \nu_{FSR} \approx 2\,\text{GHz}$. The Scale Factor readout senses the offset $\Delta\hat{\nu}_{FSR} = \Upsilon_{FSR} - \nu_{FSR}$ between the FSR sub-carriers and their associated upper/lower resonances by an angle modulation at a unique MHz-scale 'SF tone'. This additional nested angle-modulation provided by the SF tone generates phase modulation side bands about each FSR sub-carrier, but *not* at the carrier frequency of the laser.

Detuning of the FSR sub-carriers relative to their respective cavity resonances results from a change in cavity FSR and, accordingly, a change in Scale Factor. This change is measured via a mechanism analogous to PDH, where interaction of the FSR sub-carrier with the cavity response causes phase rotation of the sub-carrier relative to the non-resonant sideband modulation. For this reason the SF tone frequency is selected to be greater than the cavity linewidth. The sub-carrier phase rotation provides conversion of Phase to Amplitude modulation for subsequent lock-in detection. Since the SF readout is referenced to the USO, uncontrolled changes in the FSR

Optics EXPRESS

modulation frequency due to USO drift will mimic scale factor changes, however correction is readily available by tracking the absolute USO frequency against e.g. GPS timestamps as part of regular mission function [10].

Practically, the LRP's PDH output can be summed with the FSR waveform within the SFU prior to the cavity's phase modulator. Linearity of the phase modulator (voltage) input means that the waveform summation is equivalent to independent, series modulators drive by the respective PDH and FSR waveforms, and eliminates the need for a second (new) modulator. Further, the SF tone frequency Υ_{SF} is selected as $\Upsilon_{SF} \neq \Upsilon_{PDH}$ to differentiate it from PDH modulation frequency.

The electric field of the light exiting the optical phase modulator is given by

$$E(t) = E_0 e^{i\omega_0 t} \underbrace{e^{i\alpha \sin(2\pi \Upsilon_{\mathrm{PDH}} t)}}_{\mathrm{PDH}} \underbrace{e^{i\beta \sin(2\pi \Upsilon_{\mathrm{FSR}} t + \gamma \sin(2\pi \Upsilon_{\mathrm{SF}} t))}}_{\text{Scale Factor}} \tag{3}$$

where E_0 is the input field amplitude, ω_0 is the laser carrier frequency, Υ_{PDH} [Hz] is the PDH frequency with associated modulation depth α [rad], Υ_{FSR} [Hz] is the FSR tone modulation with modulation depth β [rad], and Υ_{SF} [Hz] is SF frequency of angle modulation applied to the FSR tone waveform, with depth γ [rad]. To first order, the field can be expanded as:

$$\begin{aligned} E(t) = E_0\, e^{i\omega_0 t} \Bigg\{ & J_0(\alpha)J_0(\beta) + \underbrace{J_0(\beta)J_1(\alpha)e^{i2\pi \Upsilon_{\mathrm{PDH}} t} - J_0(\beta)J_1(\alpha)e^{-i2\pi \Upsilon_{\mathrm{PDH}} t}}_{Carrier-PDH} \\ & + J_1(\beta)e^{i2\pi \Upsilon_{\mathrm{FSR}} t}\Big(J_0(\alpha)J_0(\gamma) + \underbrace{J_1(\alpha)J_0(\gamma)e^{i2\pi \Upsilon_{\mathrm{PDH}} t} - J_1(\alpha)J_0(\gamma)e^{-i2\pi \Upsilon_{\mathrm{PDH}} t}}_{Upper\ FSR-PDH} \\ & + \underbrace{J_0(\alpha)J_1(\gamma)e^{i2\pi \Upsilon_{\mathrm{SF}} t} - J_0(\alpha)J_1(\gamma)e^{-i2\pi \Upsilon_{\mathrm{SF}} t}}_{Upper\ FSR-SF}\Big) \\ & - J_1(\beta)e^{-i2\pi \Upsilon_{\mathrm{FSR}} t}\Big(J_0(\alpha)J_0(\gamma) \quad + \underbrace{J_1(\alpha)J_0(\gamma)e^{i2\pi \Upsilon_{\mathrm{PDH}} t} - J_1(\alpha)J_0(\gamma)e^{-i2\pi \Upsilon_{\mathrm{PDH}} t}}_{Lower\ FSR-PDH} \\ & - \underbrace{J_0(\alpha)J_1(\gamma)e^{i2\pi \Upsilon_{\mathrm{SF}} t} \quad + J_0(\alpha)J_1(\gamma)e^{-i2\pi \Upsilon_{\mathrm{SF}} t}}_{Lower\ FSR-SF}\Big)\Bigg\}, \end{aligned} \tag{4}$$

where $J_n(x)$ denotes the n-th Bessel function of the first kind. Here we assume that PDH and FSR modulation is small (typically <1 rad), and that higher order side bands may be ignored. This is a reasonable assumption for the modulation depths that might be expected for mission.

The resulting output of the modulator is the convolution product of the two modulations summed and injected into the phase modulator (PDH and SF). The modulation pattern is illustrated in Fig. 3. A conventional phase modulation pattern for the PDH side bands is present about both the laser fundamental frequency and FSR Gigahertz sub-carriers. Demodulation of detected photo-current at Υ_{PDH} will produce an error signal proportional to the absolute laser offset from the closest cavity fringe. Conversely, the scale factor readout side bands are only present on the FSR sub-carriers and exhibit an odd symmetry with respect to the Gigahertz products about the carrier frequency. This asymmetry inverts the demodulated lock-in signals sampled at resonances above and below the carrier, making the readout sensitive to the differential effect of mode spacing change (scale factor) and insensitive to common optical carrier frequency changes. Beat components from the resonances above and below the carrier frequency will sum coherently and when demodulated at Υ_{SF} will form a single scale factor readout proportional to $\Delta = \Upsilon_{\mathrm{FSR}} - \nu_{\mathrm{FSR}}$, with a mathematical form equivalent to that of a PDH error signal. This Scale Factor error signal samples the difference in frequency between reference oscillator tone and the

Optics EXPRESS

true frequency of the cavity FSR spacing. Thus, with a laser stabilised to a known cavity fringe and a readout of the mode spacing referenced against an external oscillator, a readout of absolute frequency drift can be made. From this, fractional frequency changes of the laser's absolute frequency can be estimated and factored into the interferometrically derived ranging signals of a GRACE-FO like instrument.

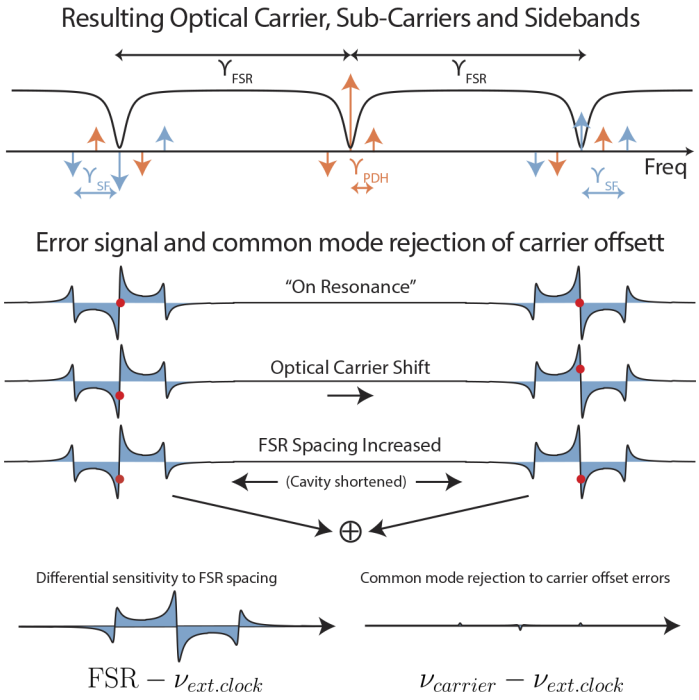

Fig. 3. Frequency-Phasor diagram of first order terms of optical modulator output. PDH sidebands have an offset frequency of Υ_{PDH} at each of the carrier and sub-carrier components. The external reference oscillator frequency Υ_{FSR} sets the sub-carrier frequency and is set close to the cavity free spectral range ν_{FSR}. To this electronics waveform an angle modulation Υ_{SF} applied to provide sidebands to readout Scale Factor (SF). An error signal is generated by demodulating at both the PDH modulation frequency (for locking to a cavity fringe) and at the scale factor modulation frequency to extract a readout out of $\Delta = \Upsilon_{\mathrm{FSR}} - \nu_{\mathrm{FSR}}$ (the change of cavity longitudinal mode spacing relative to our externally clocked reference tone). The illustration shows a modeled error signal for the scale factor readout and a scaled response of the scale factor response to carrier offset from cavity resonant fringe at the 100 Hz level.

4. Experimental verification of concept

The experimental layout used to verify this readout scheme is illustrated in Fig. 4. A single laser (1064 nm NPRO, Innolight Prometheus) was stabilised to an optical reference cavity using a conventional Pound-Drever-Hall (PDH) feedback loop [14]. Here the optical cavity was a moderate finesse (~9400) traveling wave optical cavity with an FSR of 1.78 GHz and Full Width Half Maximium (FWHM) of 190 kHz and demonstrated performance compatible with GRACE-FO requirements [17]. This cavity was constructed from Ultra Low Expansion (ULE) glass (spacer and mirrors), with a mean coefficient of thermal expansion of order 0 ± 30 ppb/°C from $5 - 35$ °C [18], and housed within a thermally isolated and controlled vacuum vessel. A Liquid Instruments Moku:Lab provided a digital PDH controller for frequency feedback to the

Optics EXPRESS

NPRO PZT and Thermal frequency control actuators. A list of further experimental parameters is provided in Table 1.

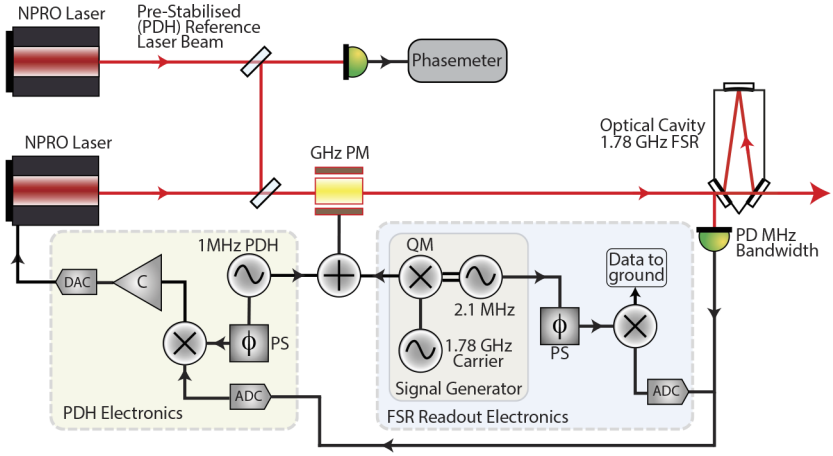

Fig. 4. Schematic of FSR readout experiment. An NPRO 1064 nm laser is locked to a resonance of a traveling wave triangular cavity using conventional Pound-Drever-Hall locking; a 1 MHz tone is used to generate phase modulation side bands that convert to amplitude (AM) as the cavity drifts off resonance, this signal is sensed on reflection by a Megahertz bandwidth photo detector and demodulated to generate an error signal that is fed back to the laser to hold it on resonance. For the FSR readout, a 1.78 GHz signal is angle modulated with a 2.1 MHz base band waveform, using a Quadrature Mixer (QM), to generate a nested modulation with the sideband pattern illustrated in Fig. 3. As the cavity free spectral range changes relative to the reference external Gigahertz carrier the upper and lower Gigahertz sidebands each convert phase modulation at 2.1 MHz into AM that is detected, digitised and demodulated within a FPGA signal processing chain. The result is an error signal similar to the well known PDH error signal, however due to the odd symmetry of the Gigahertz components around resonance it is, to first order, sensitive to changes in mode spacing rather than absolute frequency. Thus we have a pair of error signals that independently sense the absolute frequency of the laser relative to a resonance, and also the spacing of modes relative to an external non-optical absolute reference.

Table 1. List of experimental parameters

Parameter	Experimental Value
Cavity input power (P_0)	700 μ W
Laser wavelength (approx.)	1064 nm
Cavity FSR (ν_{FSR})	1.78 GHz
Cavity finesse (approx.)	9400
PDH sidebands (Υ_{PDH})	1.0 MHz
PDH sideband modulation depth (α)	0.04 rad
FSR carrier tone (Υ_{FSR})	1.78 GHz
FSR carrier modulation depth (β)	0.75 rad
Scale factor modulation tone (Υ_{SF})	2.1 MHz
Scale factor modulation depth (γ)	0.3 rad

Phase modulation was applied using a single wide-bandwidth (10 GHz) fiber coupled waveguide Lithium Niobate phase modulator (iXblue, NIR-MPX-LN-10), chosen for its low AM residuals,

Optics EXPRESS

high stability and low drive voltage requirements. The $\Upsilon_{SF} \approx 1.78$ GHz FSR tone (matched to the nominal cavity FSR), was generated using a Rhode & Schwartz SMB100B signal generator, with an internal OCXO frequency reference. The FSR tone was directly phase modulated within the signal generator with the sinusoidal SF tone of 0.3 rad applied at $\Upsilon_{SF} = 2.1$ MHz. An RF resistive combiner component (Mini-Circuits ZFRSC-42-S+) was used for waveform summation for (~MHz) PDH and (~GHz) FSR electronic voltage waveforms.

Modulated light was mode matched into the optical cavity and the reflected field detected on an InGaAs 150 MHz bandwidth fixed gain photodetector (Thorlabs PDA05CF2). A digital lock-in amplifier running on a second Liquid Instruments Moku:Lab FPGA unit was used to demodulate and log the Scale Factor measurement. This mixed the reflected photodetector signal with a 2.1 MHz tone derived from the Gigahertz FSR signal generator, low pass filtered with a 10.1 Hz 18 dB/oct filter and digitally amplified by +90 dB gain before being logged to disk. A calibration of the scale factor slope sensitivity around the zero crossing point (e.g. 0 Hz FSR estimation error) was carried out by stepping the FSR tone by a series of 10 Hz offsets, resulting in a calibration coefficient of 230 Hz/V which was used to scale the logged data [V] into input referred FSR frequency detuning [Hz].

An example sweep of the SF readout signal was obtained by sweeping the FSR tone over a 6 MHz range about the nominal cavity FSR. The resulting readout is shown in Fig. 5, demonstrating the near linear sensitivity to FSR tone frequency error (recorded with +40 dB Gain). On orbit, the FSR detuning is expected to have very small signal dynamics over mission lifetime of $\delta\nu_{FSR}/\nu_{FSR} \sim 10^{-7}$ or $\delta\nu_{FSR} \sim 200$ Hz, as estimated from the published scale factor data for GRACE-FO [13,19]. For this reason, data acquisition was performed with an optimized +90 dB gain which provided a narrow-but-sufficient (unsaturated) measurement range of ±100 Hz within the linear region around the true FSR.

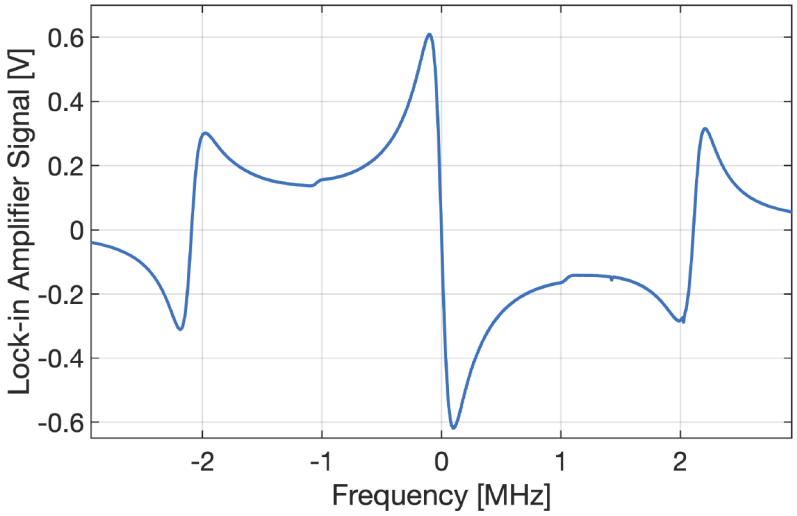

Fig. 5. Example sweep of FSR readout signal as a function of external reference oscillator frequency. Here gain of the lock-in amplifier was reduced to +40 dB (from +90 dB) to allow us to see the full peak-to-peak of the error signal within the dynamic range of the instrument. Reported 'Volts' are in equivalent units of the Moku:Lab input ADC. The following measurements presented in this Section utilise only narrow ±100 Hz linear region of the signal about the center zero crossing point. A slight asymmetry is observed in the upper and lower single-sideband components of the error signal sweep due to the modulation frequency being within an order of magnitude of the reference cavity linewidth.

Optics EXPRESS

The FSR readout signal was recorded for a period of 30 days, during which time our laboratory remained undisturbed. The resulting calibrated readout signal of cavity mode spacing showed the relative stability of the passive thermally isolated cavity against the frequency reference provided by our signal generator. The full time series data for this 30 day period is given in Fig. 6. The fractional frequency change during this time period did not exceed 10^{-8}.

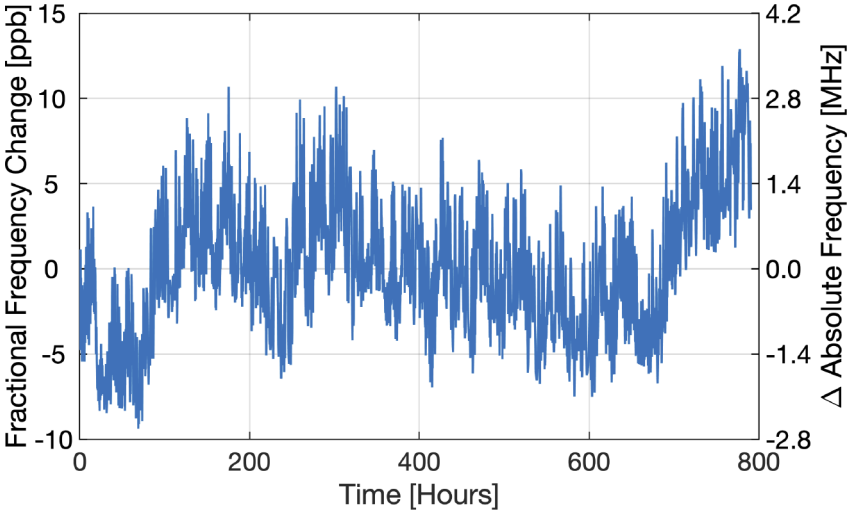

Fig. 6. Full time series data; 800 hours represents 33 days of unbroken data. The cavity temperature was not actively controlled for this measurement. The fractional frequency change shown in this measurement does not exceed ±10 ppb. This demonstrates performance an order of magnitude better than the current scale factor for GRACE-FO (10^{-7}).

The Allan Deviation of the FSR readout data is shown in Fig. 7, achieving performance an order of magnitude below the expected next mission requirement. For comparison, a PDH readout with two lasers locked to a single cavity one FSR apart is also plotted, as is an external clock measurement which shows the FSR readout is not limited by clock noise.

To verify the frequency stabilization performance is not impacted by the scale-factor readout, a tap-off of the laser was interfered with a second, independent laser stabilised to a second reference optical cavity on a high-bandwidth photo-detector. The relative frequency of the two lasers was tracked using a digital phasemeter (Liquid Instruments, Moku:Lab). Figure 8 shows this beatnote measurement, taken simultaneously with an FSR readout measurement, is able to be maintained below the GRACE-FO mission requirement curve.

Whilst the measured changes are comparable to the anticipated on-orbit environment (fractional changes ~ 10^{-8}), the absence of an external absolute frequency reference (see Section 5.) requires a dedicated test to verify the readout sensitivity to FSR (& scale factor) changes over other potentially confounding factors, such as electronics noise and reference oscillator drift. To accomplish this, a 5°C step/offset was added to the optical cavity's thermal set-point of the cavity's thermal shield enclosure to induce change in cavity FSR via thermal expansion. The corresponding change in FSR readout is presented in Fig. 9, from which an estimated ~12 ppb/°C fractional length change has occurred in the cavity (within the 0 ± 30 ppb/°C expected from the ULE spacer material at 5-35°C [18]). Accurate measurement of the FSR change verifies the method's sensitivity to a scale-factor perturbation.

Optics EXPRESS

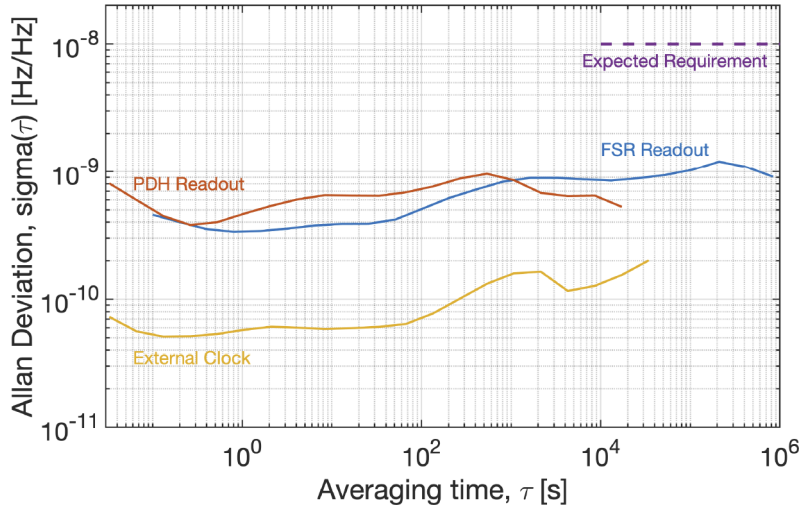

Fig. 7. Measured Allan deviation of frequency readout relative to stable Oven Controlled Oscillator (OCOX) reference and PDH readout. The FSR readout is performing an order of magnitude below the expected next mission requirement, and is not limited by clock noise.

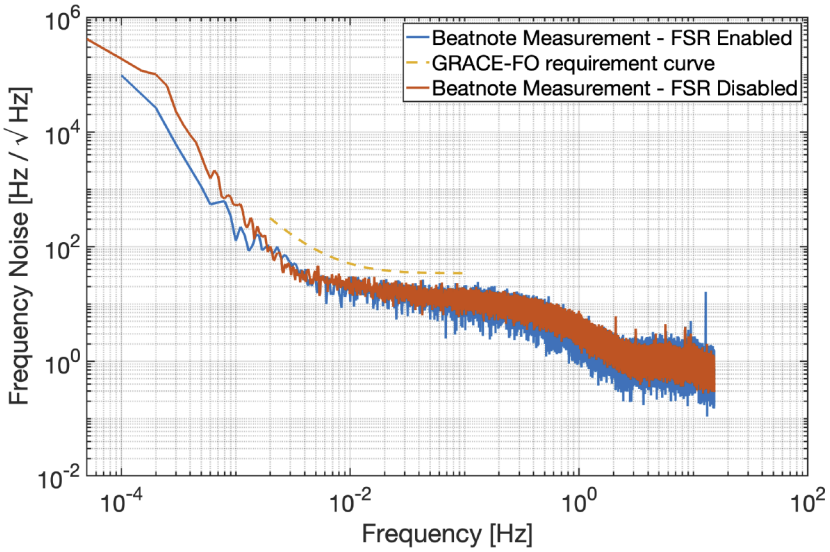

Fig. 8. Frequency noise $[Hz/\sqrt{Hz}]$ of the beatnote of two cavity stabilised lasers. The two traces show the performance with (blue) and without (orange) the FSR readout (GHz sidebands) enabled - showing the primary (PDH) laser stabilisation system meets performance requirements in either case. The frequency noise is calculated by taking the square root of the Power Spectral Density (PSD), and is also referred to as the root psd or rpsd.

Optics EXPRESS

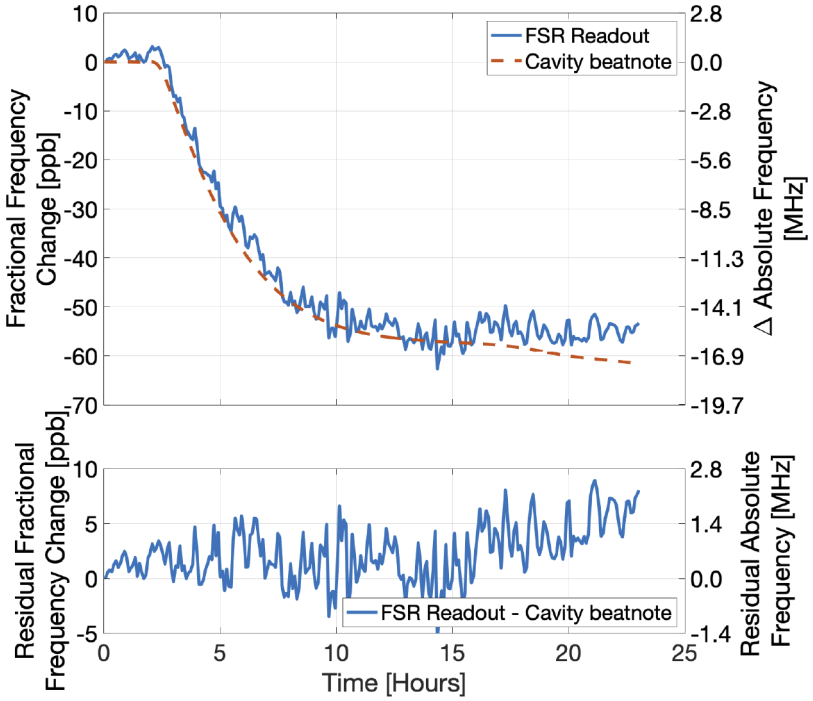

Fig. 9. Cavity Temperature step test. A temperature step of +5 °C was applied, and a corresponding change in the readout equivalent to 12 ppb/°C of fractional length change of the cavity is seen. This demonstrates that the readout responds to the changes in the optical setup and is not just an artifact of reference oscillator drift or electronic readout drift. The cavity beatnote was used as verification of the FSR readout, with much higher precision.

5. Discussion

5.1. Open-loop vs closed-loop operation

The results presented here show sufficient performance to meet expected mission requirements in *open-loop monitoring* of FSR changes, as the estimated FSR carrier frequency is kept constant throughout the measurement. However, long-term systematic drift will introduce a static offset of the FSR sub-carriers from resonance, which can increase the coupling of noise sources such as laser intensity noise. On the other hand *closed-loop tracking*, where the FSR estimate is updated on a quasi-continuous basis can be used to continuously null the FSR estimation error, potentially delivering improved performance. Similarly, residual amplitude modulation (RAM) introduced by the electro-optic modulator (EOM) can also introduce offsets of the FSR sub-carriers from resonance. When characterised for this system there was no significant RAM at the scale factor modulation frequency due to the fact that there is no modulation signal driven to the EOM at this frequency. Further, the effects of RAM would affect closed and open loop implementations equally. Answering this question will be the subject of future work, however the authors note that the dynamics anticipated to affect the scale-factor likely occur at the time scale of days (thermal) or longer (aging), indicating that semi-regular/periodic update of the FSR frequency via OBC/ground-command will likely be sufficient if further investigation reveals noise coupling to be a limiting factor in scale-factor determination.

Optics EXPRESS

5.2. Verifying absolute frequency

This paper has discussed the frequency readout scheme as absolute. During the commissioning and initial acquisition of the GRACE-FO LRI link, the lasers were successfully locked to their respective optical cavity with negligible deviation from ground-calibrated offsets [6]. This indicates that neither the laser nor cavities experienced a significant shift in emission or resonant mode frequencies during launch. For future missions, should such a shift occur, the absolute optical frequency can be estimated in orbit by comparison of the laser range measurement with an independent range, likely provided by GPS position information. For GRACE-FO, a ≈1000 m time-varying relative-range signal exists at the orbital frequency due to the orbit mismatch and other effects. On board differential-GPS measurements are estimated to measure the inter-spacecraft range with $<700\,\mu m$ precision [20], providing better than $<1\,\mathrm{mm}/1\,\mathrm{km} \approx 1:10^6$ fractional uncertainty. Such uncertainty is sufficient to resolve the 282 THz laser frequency to within 300 MHz, well below the cavity FSR of ≈2 GHz, such that the cavity mode number n_{mode}, and therefore absolute laser frequency, can be unambiguously determined.

5.3. Demodulation phase

The proposed implementation illustrated in Fig. 2 shows a dashed line showing an optional phase synchronisation between the LRP FSR firmware and the SF NCO. Should the phase synchronisation not be implemented, the FSR readout becomes sensitive to any phase or frequency drift/offsets between the LRP and SF NCOs. Synchronisation of the LRP and SF NCOs to a fraction of the SF modulation frequency (Megahertz) would require timing synchronisation of better than <100 nano-seconds, which is un-achievable with the micro-second synchronization provided by the GRACE-FO 'pulse-per-second' timing reference distributed to modules. Instead, the SF data can be streamed to the ground from both lock-in demodulation quadratures (cosine and sine), allowing for the correct phase to be determined in post processing. Verification of dual-quadrature readout, long with the specification of any associated calibration signals will be addressed in future work.

6. Conclusions

Laser-only geodesy missions will require a new method to track long term changes in laser frequency to provide coherence of measured range data over multi-year mission lifetimes. The readout technique proposed in this paper offers an elegant method of determining fractional frequency (or length) changes of a stabilised laser (cavity) against an external ultra-stable external standard (USO). When coupled with calibration knowledge of the cavity mode number, the results presented here experimentally demonstrated at a fractional absolute laser frequency stability at $<10^{-9}$ over a 30 day measurement, exceeding the anticipated 10^{-8} specification for future satellite-geodesy missions. Further, the presented readout scheme introduces minimal additional parts to the flight heritage GRACE-FO LRI baseline design, with the addition of Gigahertz bandwidth parts only in the waveform synthesizer and a high speed modulator (no major LRP modifications are anticipated).

Funding. Australian Research Council (OzGrav CE170100004, EQUS CE170100009); Australian Government Research Training Program (RTP Scholarship); Jet Propulsion Laboratory (NASA JPL/Caltech).

Disclosures. The authors declare no conflicts of interest.

Data availability. Data underlying the results presented in this paper are not publicly available at this time but may be obtained from the authors upon reasonable request.

References

1. B. D. Tapley, S. Bettadpur, J. C. Ries, P. F. Thompson, and M. M. Watkins, "GRACE measurements of mass variability in the Earth system," Science **305**(5683), 503–505 (2004).

Optics EXPRESS

2. R. P. Kornfeld, B. W. Arnold, M. A. Gross, N. T. Dahya, W. Klipstein, P. F. Gath, and S. Bettadpur, "GRACE-FO: The Gravity Recovery and Climate Experiment Follow-On Mission," J. Spacecr. Rockets **56**(3), 931–951 (2019).
3. National Academies of Sciences, Engineering and Medicine, *Thriving on Our Changing Planet: A Decadal Strategy for Earth Observation from Space* (National Academies, 2018).
4. J. Conklin, T. Yu, F. Guzman, B. Klipstein, J. Lee, J. Leitch, K. Numata, S. Petroy, R. E. Spero, B. Ware, and G. Yang, "LRI Technology Summary and Roadmap for Mass Change Mission, May 2020," Tech. rep., NASA Jet Propulsion Laboratory, (2020).
5. K. Nicklaus, S. Cesare, L. Massotti, L. Bonino, S. Mottini, M. Pisani, and P. Silvestrin, "Laser metrology concept consolidation for NGGM," CEAS Space J. **12**(3), 313–330 (2020).
6. K. Abich, A. Abramovici, B. Amparan, A. Baatzsch, B. B. Okihiro, D. C. Barr, M. P. Bize, C. Bogan, C. Braxmaier, M. J. Burke, K. C. Clark, C. Dahl, K. Dahl, K. Danzmann, M. A. Davis, G. de Vine, J. A. Dickson, S. Dubovitsky, A. Eckardt, T. Ester, G. F. Barranco, R. Flatscher, F. Flechtner, W. M. Folkner, S. Francis, M. S. Gilbert, F. Gilles, M. Gohlke, N. Grossard, B. Guenther, P. Hager, J. Hauden, F. Heine, G. Heinzel, M. Herding, M. Hinz, J. Howell, M. Katsumura, M. Kaufer, W. Klipstein, A. Koch, M. Kruger, K. Larsen, A. Lebeda, T. Leikert, C. C. Liebe, J. Liu, L. Lobmeyer, C. Mahrdt, T. Mangoldt, K. McKenzie, M. Misfeldt, P. R. Morton, V. Muller, A. T. Murray, D. J. Nguyen, K. Nicklaus, R. Pierce, J. A. Ravich, G. Reavis, J. Reiche, J. Sanjuan, D. Schutze, C. Seiter, D. Shaddock, B. Sheard, M. Sileo, R. E. Spero, G. Spiers, G. Stede, M. Stephens, A. Sutton, J. Trinh, K. Voss, D. Wang, R. T. Wang, B. Ware, H. Wegener, S. Windisch, C. Woodruff, B. Zender, and M. Zimmermann, "In-Orbit Performance of the GRACE Follow-on Laser Ranging Interferometer," Phys. Rev. Lett. **123**(3), 031101 (2019).
7. K. Ghobadi-Far, S. C. Han, C. M. McCullough, D. N. Wiese, D. N. Yuan, F. W. Landerer, J. Sauber, and M. M. Watkins, "GRACE Follow-On Laser Ranging Interferometer Measurements Uniquely Distinguish Short-Wavelength Gravitational Perturbations," Geophys. Res. Lett. **47**(16), e2020GL089445 (2020).
8. NASA, "ORCLS - Optical-Radio Coherence for Laser Stability," https://techport.nasa.gov/view/94040.
9. R. G. DeVoe and R. G. Brewer, "Laser-frequency division and stabilization," Phys. Rev. A **30**(5), 2827–2829 (1984).
10. H. Y. Wen, G. Kruizinga, M. Paik, F. Landerer, W. Bertiger, C. Sakumura, T. Bandikova, and C. Mccullough, "Gravity recovery and climate experiment follow-on (GRACE-FO) level-1 data product user handbook," JPL D-56935 (URS270772) **11**, (2019).
11. G. Weaver, M. Reinhart, and R. Wallis, "Enhancing the art of space operations-progress in JHU/APL ultra-stable oscillator capabilities," in *Proceedings of the 40th Annual Precise Time and Time Interval Systems and Applications Meeting* (2008), pp. 57–68.
12. B. Bachman, G. de Vine, J. Dickson, S. Dubovitsky, J. Liu, W. Klipstein, K. McKenzie, R. E. Spero, A. J. Sutton, B. Ware, and C. Woodruff, "Flight phasemeter on the Laser Ranging Interferometer on the GRACE Follow-On mission," J. Phys.: Conf. Ser. **840**, 012011 (2017).
13. M. Misfeldt, V. Muller, H. Wegener, L. Muller, and G. Heinzel, "Scale factor of the laser ranging interferometer in GRACE follow-on," GRACE Science Team Meeting, (2020).
14. R. W. P. Drever, J. L. Hall, F. V. Kowalski, J. Hough, G. M. Ford, A. J. Munley, and H. Ward, "Laser phase and frequency stabilization using an optical resonator," Appl. Phys. B **31**(2), 97–105 (1983).
15. T. T. Y. Lam, B. J. J. Slagmolen, J. H. Chow, I. C. M. Littler, D. E. McClelland, and D. Shaddock, "Digital Laser Frequency Stabilization Using an Optical Cavity," IEEE J. Quantum Electron. **46**(8), 1178–1183 (2010).
16. R. Thompson, W. M. Folkner, G. de Vine, W. Klipstein, K. McKenzie, R. E. Spero, N. Yu, M. Stephens, J. Leitch, R. Pierce, T. T. Y. Lam, and D. Shaddock, "A flight-like optical reference cavity for GRACE follow-on laser frequency stabilization," in *2011 Joint Conference of the IEEE International Frequency Control and the European Frequency and Time Forum (FCS) Proceedings* (2011), pp. 1–3.
17. N. Chabbra, A. R. Wade, E. R. Rees, A. J. Sutton, A. Stochino, R. L. Ward, D. A. Shaddock, and K. McKenzie, "High stability laser locking to an optical cavity using tilt locking," Opt. Lett. **46**(13), 3199–3202 (2021).
18. Incorporated Corning, 7972 ULE Product Information https://www.corning.com/media/worldwide/csm/documents/7972%20ULE%20Product%20Information%20Jan%202016.pdf (2016).
19. GRACE-FO Level 1A/B data is available at http://podaac.jpl.nasa.gov.
20. D. Gu, B. Ju, J. Liu, and J. Tu, "Enhanced GPS-based GRACE baseline determination by using a new strategy for ambiguity resolution and relative phase center variation corrections," Acta Astronaut. **138**, 176–184 (2017).